Mathematical Biosciences and Engineering

MBE, 21(4): 5536–5555.
DOI: 10.3934/mbe.2024244
Received: 05 January 2024
Revised: 28 February 2024
Accepted: 05 March 2024
Published: 27 March 2024

http://www.aimspress.com/journal/MBE

Research article

Mechanistic modeling of alarm signaling in seed-harvester ants

Michael R. Lin[1], Xiaohui Guo[2,*], Asma Azizi[3], Jennifer H. Fewell[4] and Fabio Milner[1,5]

[1] Simon A. Levin Mathematical, Computational and Modeling Sciences Center, Arizona State University, Tempe 85281, USA
[2] Department of Physics of Complex Systems, Weizmann Institute of Science, Rehovot 7632706, Israel
[3] Department of Mathematics, Kennesaw State University, Marietta 30062, USA
[4] School of Life Sciences, Arizona State University, Tempe 85287, USA
[5] School of Mathematical and Statistical Sciences, Arizona State University, Tempe 85287, USA

* **Correspondence:** Email: xiaohui.guo@weizmann.ac.il.

Supplementary

The empirical data from [1] is utilized to estimate the model parameters. In this supplementary file, we present both empirical and estimated distributions for certain model parameters, such as the anticipated speed of ants and their turning angles.

A group of N ant workers navigates a 2D circular arena with a radius of M = 520 pixels in continuous space, see Figure S1.

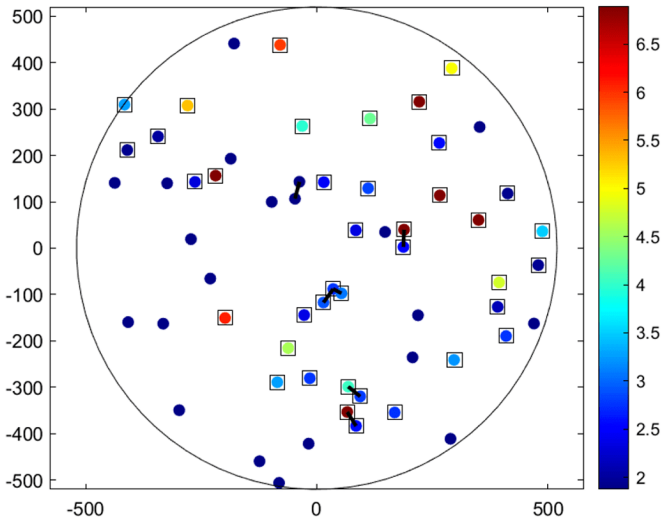

Figure S1. A single frame extracted from the simulation utilizing the baseline parameters in Table 1 in the main text: The color scheme illustrates the current speed parameter, λ_t^p in pixels per time-step, for each agent. Visual segments connect pairs of agents currently in contact, and boxed points draw attention to agents in the alarmed state. For a more dynamic presentation, kindly refer to the Supplemental Videos.

The angle of the ant's heading during time-step t, denoted by θ_t^p, defined as the counterclockwise angle from the x-axis of the vector connecting two consecutive positions as shown in Figure S2.

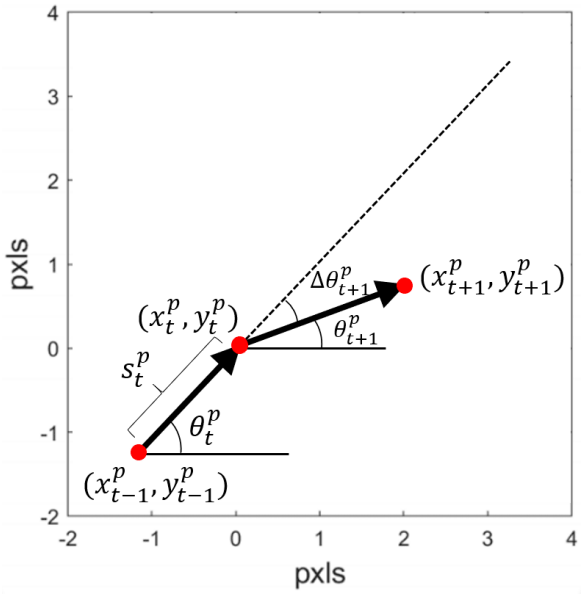

Figure S2. Position update notation at time-step t: The axes depict Cartesian space within the model, with the model's length scale adjusted to match empirical tracking data. Since the tracking data is quantized into a pixel-based coordinate system, each unit in the model arena equates to a length of 1 pixel.

The change in heading, denoted as $\Delta\theta_t^p = \theta_t^p - \theta_{t-1}^p$, is observed to adhere to a Laplace distribution, as illustrated by the black curve in Figure S3. Consequently, we have employed the following distribution fitting to the data:

$$P(\Delta\theta_t^p) = \frac{\omega \exp(-\omega|\Delta\theta_t^p|)}{2}, \Delta\theta_t^p \epsilon(-\pi, \pi), \tag{S1}$$

here, ω^{-1} represents the mean magnitude of the turning angle, which remains consistent for all ants across all time-steps, as depicted by the red curve in Figure S3.

Based on the data visualization, it appeared to us that the exponential distribution is a suitable fit. When fitting this distribution to the data, the goodness of fit was deemed acceptable, with a sum of squared errors (SSE) of 10^{-4} and an adjusted R-square of 0.98.

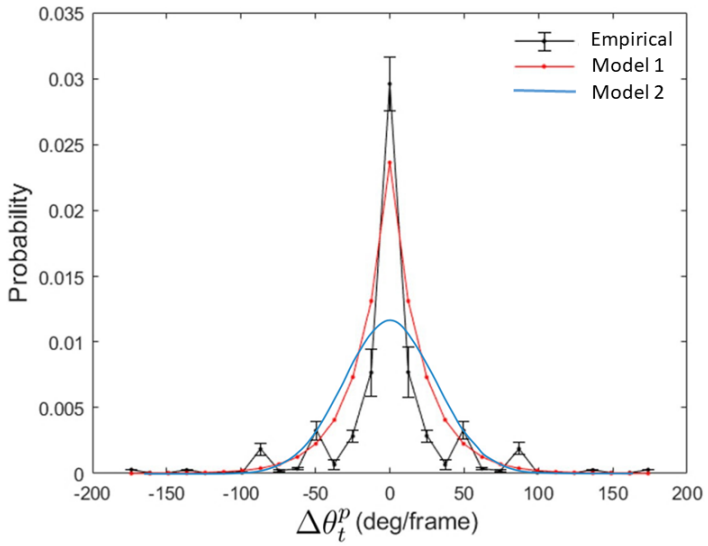

Figure S3. Distribution of turning angles $\Delta\theta$ from empirical data and the models: The black histogram depicts the aggregated data from all three post-introduction empirical videos. Error bars indicate the standard error of the mean across these three videos. Smaller peaks in the empirical distribution are attributed to the quantization of spatial coordinates in the tracking data based on pixel locations. The red curve represents the model of Laplace probability distribution of turning angles at each time-step (RMSE = 0.00036). This distribution was adjusted to match the empirical distribution using Eq (S1) with $\omega^{-1} = 21.4^{\circ}$. The blue curve depicts a model of normal probability distribution of turning angles at each time-step (RMSE = 0.00393).

The empirical data indicates that the speed of ant *p* at time *t*, denoted as s_t^p depicted by the black curve in Figure S4. Based on this data visualization, it appears that the exponential distribution is a suitable fit. We employ the distribution in Eq (S2) to analyze the data and determine the expected speed for ant *p* at time *t*, denoted as λ_t^p. Fitting this distribution to the data, the goodness of fit is deemed acceptable, with a sum of squared errors (SSE) of 10^{-4} and an adjusted R-square of 0.98. The curve obtained from the fitting process is illustrated as the red curve in Figure S4.

$$P\left(s_t^p\right) = \frac{exp\left(-\frac{s_t^p}{\lambda_t^p}\right)}{\lambda_t^p}. \tag{S2}$$

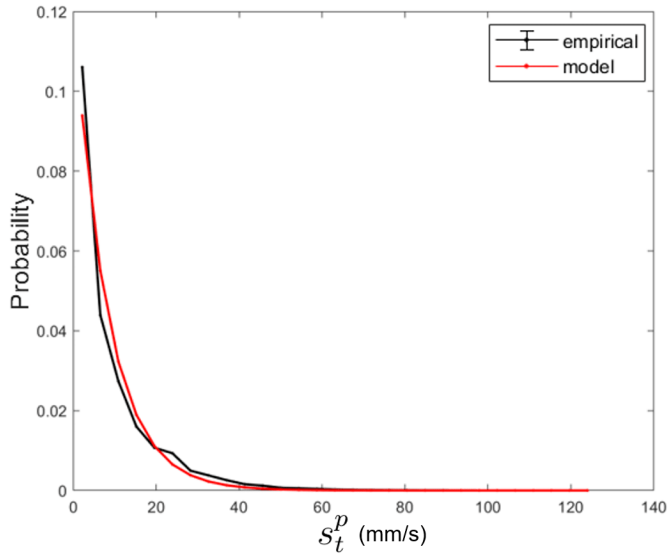

Figure S4. Comparison between the framewise speed distribution observed in empirical videos and the model's specified speed distribution for an individual ant: The black curve represents the amalgamation of all videos recorded prior to stimulus introduction, encompassing all individuals across various videos and times without alarm stimuli. On the other hand, the red curve is the result of fitting the exponential probability distribution (following Eq (S2), with λ^* set at 1.87 pixels per time-step) to the black curve. This determined best-fit value was consistently applied in all model simulations to define the framewise speed distribution of unalarmed ants, unless explicitly stated otherwise. It's important to note that for alarmed ants, characterized by λ_t^p values different from λ^*, the red curve would exhibit a thicker tail compared to the observed empirical curve.

References

1. X. Guo, M. R. Lin, A. Azizi, L. P. Saldyt, Y. Kang, T. P. Pavlic, et al., Decoding alarm signal propagation of seed-harvester ants using automated movement tracking and supervised machine learning, *Proc. R. Soc. B*, **289** (2022), 20212176. https://doi.org/10.1098/rspb.2021.2176